

PRELIMINARY RECONSTRUCTIONS OF SPRING PRECIPITATION IN SOUTHWESTERN TURKEY FROM TREE-RING WIDTH

RAMZI TOUCHAN,^{a,*} GREGG M. GARFIN,^b DAVID M. MEKO,^a GARY FUNKHOUSER,^a NESAT ERKAN,^c
MALCOLM K. HUGHES^a and BRIAN S. WALLIN^a

^a *Laboratory of Tree-Ring Research, The University of Arizona, PO Box 210058, Tucson, Arizona 85721-0058, USA*

^b *Institute for the Study of Planet Earth, The University of Arizona, Tucson, Arizona 85721-0156, USA*

^c *Southwest Anatolia Forest Research Institute (SAFRI), POB:264, Antalya, Turkey*

Received 5 February 2002

Revised 19 July 2002

Accepted 22 July 2002

ABSTRACT

Two reconstructions of spring (May–June) precipitation have been developed for southwestern Turkey. The first reconstruction (1776–1998) was developed from principal components of nine chronologies of *Cedrus libani*, *Juniperus excelsa*, *Pinus brutia*, and *Pinus nigra*. The second reconstruction (1339–1998) was derived from principal components of three *J. excelsa* chronologies. Calibration and verification statistics of both reconstructions indicate reasonably accurate reconstruction of spring precipitation for southwestern Turkey, and show clear evidence of multi-year to decadal variations in spring precipitation. The longest period of reconstructed spring drought, defined as consecutive years with less than 80% of normal May–June precipitation, was 4 years (1476–79). Only one drought event of this duration has occurred during the last six centuries. Monte Carlo analysis indicates a less than 33% probability that southwestern Turkey has experienced spring drought longer than 5 years in the past 660 years. Apart from the 1476–79 extended dry period, spring droughts of 3 years in length have only occurred from 1700 to the present. The longest reconstructed wet period, defined as consecutive years with more than 120% of normal May–June precipitation, was 4 years (1532–35). The absence of extended spring drought during the 16th and 17th centuries and the occurrence of extended wet spring periods during these centuries suggest a possible regime shift in climate. Preliminary analysis of links between large-scale climatic variation and these climate reconstructions shows that there is a relationship between extremes in spring precipitation and anomalous atmospheric circulation in the region. Copyright © 2003 Royal Meteorological Society.

KEY WORDS: dendrochronology; dendroclimatic reconstruction; drought; synoptic climatology analysis; NAO

1. INTRODUCTION

Turkey is the source of the rivers that provide water for many countries in the Near East, a region of prime geopolitical and historical importance. Water is the cornerstone of agricultural viability and political stability there, where strife is endemic, and competition over scarce water supplies looms as a potential flash point for all countries sharing this resource. Records of climate variability for Turkey are very short. Few of the continuous high-quality instrumental records start before the 1920s, and so the record contains only limited information on variability over decades and none for longer periods. Unfortunately, only in Western Europe and a few other regions is the instrumental record long enough to study decade-to-century-scale climate variability (Luterbacher *et al.*, 1999). To obtain records of centennial to millennial length, we need to use indirect (or proxy) evidence of climatic variability. Examples of indirect evidence range from historical documents, such as diaries recording specific weather events, to naturally formed archives, such as annual layers in corals, annual laminations in lacustrine and marine sediments, and the annual rings of trees. To

* Correspondence to: Ramzi Touchan, Laboratory of Tree-Ring Research, The University of Arizona, PO Box 210058, Tucson, Arizona 85721-0058, USA; e-mail: rtouchan@ltrr.arizona.edu

our knowledge, there have been no annual resolution precipitation reconstructions for Turkey. Many studies have demonstrated that tree-ring series can be used to reconstruct over several centuries, and occasionally millennia, past variations in precipitation, temperature, soil moisture, streamflow, the frequency of extreme droughts, and atmospheric circulation indices.

Dendrochronology has previously been applied in Turkey for the purpose of dating archaeological sites. Bannister (1970), in the first systematic attempt at tree-ring dating of Near East archaeological sites, collected and analysed tree-ring specimens from an 8th century BC tomb in Turkey. Others have since conducted extensive dendroarchaeological work in Turkey and Greece (Kuniholm and Striker, 1987; Kuniholm, 1990, 1994).

Few studies using tree rings as records of past climate (dendroclimatology) have been done in Turkey. Gassner and Christiansen-Weniger (1942) showed a clear relationship between ring widths in *Pinus nigra* and precipitation on the north-central Anatolian plateau. Akkemik (2000) investigated the response of *Pinus pinea* tree-ring width in Istanbul–Alemdağ with temperature and precipitation. Hughes *et al.* (2001) demonstrated that the crossdating in archaeological specimens over large distances in Greece and Turkey has a clear climatological basis, with signature years consistently associated with specific, persistent circulation anomalies. However, no dendroclimatic reconstruction of precipitation is currently available for Turkey.

In this paper we: (1) develop tree-ring chronologies of *Cedrus libani*, *Juniperus excelsa*, *P. nigra*, and *Pinus brutia*; (2) examine interrelationships and correlation among the chronologies; (3) study the effect of climate on tree-ring growth; (4) develop tree-ring reconstructions of climate over the past several centuries for this region; and (5) conduct a preliminary examination of links between large-scale climate and reconstructed climate.

2. SITE DESCRIPTION

Eight tree-ring sites were sampled in the Antalya and Burdur districts in southwestern Turkey near the eastern end of the Mediterranean Sea (Table I and Figure 1). Sampled sites range in elevation from 887 to 2022 m. Well-drained sites with thin soil cover were preferred in sampling to maximize likely sensitivity to drought. Soils at the sampled sites are quite different, as described in Appendix A. The study areas are characterized by Mediterranean subhumid to humid climates. Climate at the Göller (GOL) site is considered intermediate between Mediterranean and Continental regimes, with dry summers and wet winters. All of the sites in the Burdur district are in the Mediterranean Mountainous Region, and are characterized by cooler and wetter conditions than the other sites. Most of the sites are covered with snow from December to April. Generally, precipitation occurs during the autumn, winter, and spring, with a fairly dry summer (Figure 2). Mean annual precipitation ranges from 700 to 1000 mm (Turkish Ministry of Forestry, 1997; Turkish General Directorate of Meteorology, 2001).

Mean annual temperature ranges from 6 to 12 °C. July is the hottest month, with an average mean temperature from 18 to 23 °C. January is the coldest month, with an average mean temperature from –2.5 to 3.1 °C (Turkish Ministry of Forestry, 1997; Turkish General Directorate of Meteorology, 2001).

The dominant tree species at the sampled sites are shown in Table I. We sampled different species in order to establish which were suitable for crossdating and palaeoclimatological analysis.

3. METHODS AND DATA PROCESSING

3.1. Ring-width data

During 2000, the first year of sampling, nine chronologies were collected from the eight sites in the Antalya and Burdur district in Turkey (Table I and Figure 1). Increment cores were taken at all sites and full cross-sections were taken from stumps of cedar and juniper. Samples were fine-sanded and crossdated in the laboratory using standard dendrochronological techniques (Stokes and Smiley, 1968; Swetnam *et al.*, 1985).

Table I. Site information for Antalya and Burdur districts, Turkey

Site name	Site code	Species	Elevation (m)	Latitude	Longitude	Time span (year)		Total no of years	No. of trees	No. of cores
						Earliest	Latest			
Su Batan	SUB	<i>J. excelsa</i>	1808–1916	37°25'N	30°18'E	1246	2000	755	24	23
Aziziye	AZY	<i>P. nigra</i>	1601–70	37°25'N	30°17'E	1772	2000	229	13	34
Dumali Dağ	DUD	<i>P. brutia</i>	887–1426	37°24'N	30°38'E	1813	2000	188	9	14
Katrandagi	KAT	<i>C. libani</i>	1421–1517	37°23'N	30°36'E	1693	2000	308	16	26
Göller	GOLP	<i>P. brutia</i>	1002–93	37°09'N	30°31'E	1730	2000	271	11	18
Göller	GOLJ	<i>J. excelsa</i>	1002–93	37°05'N	30°31'E	1152	2000	849	17	31
Kozlu Pinari	KOP	<i>P. nigra</i>	1597–1669	36°39'N	32°12'E	1586	2000	415	16	24
Yellic Beli	YEB	<i>C. libani</i>	1668–1779	36°39'N	32°11'E	1628	2000	373	16	24
Elmali	ELMJ	<i>J. excelsa</i>	1853–2022	36°36'N	30°01'E	1332	2000	669	26	36
Elmali	ELMC	<i>C. libani</i>	1853–2022	36°36'N	30°01'E	1449	2000	552	25	36

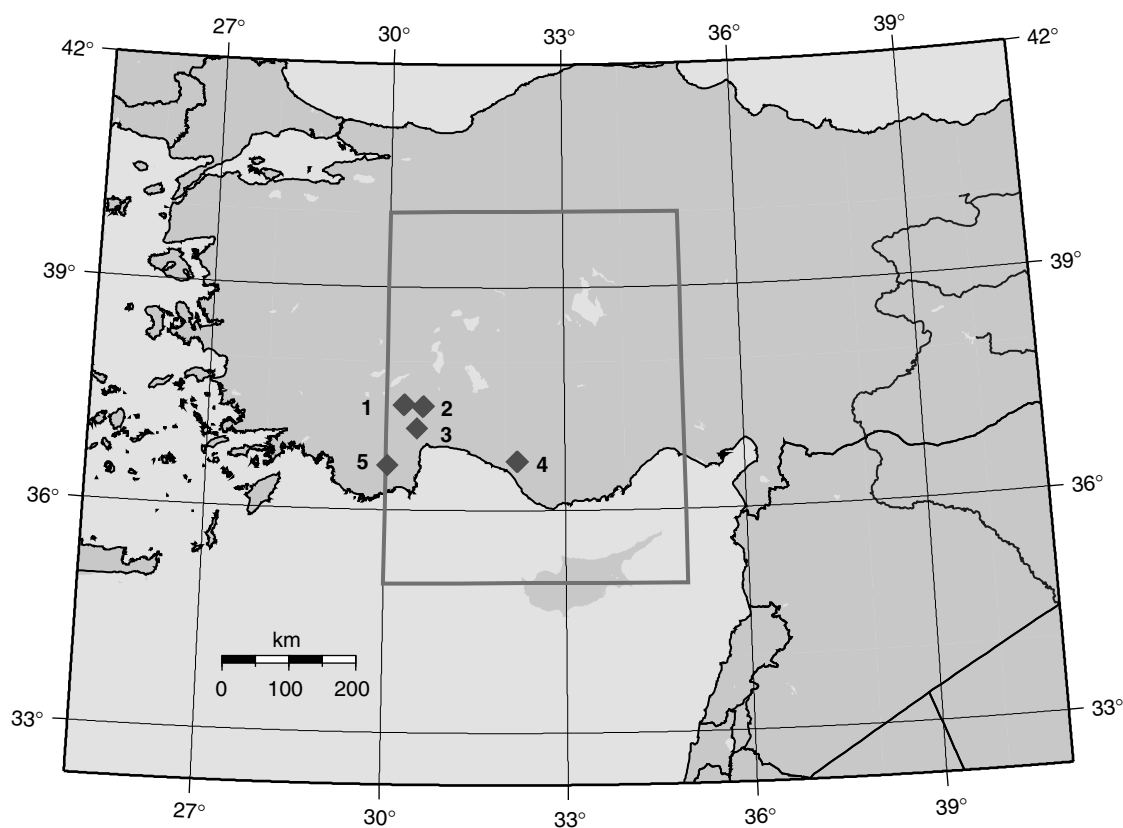


Figure 1. Locations of tree-ring sites (◆). The numbers represent groups of sites (1 = SUB and AZY, 2 = DUD and KAT, 3 = GOL, 4 = KOP and YEB, and 5 = ELMJ and ELMC). Solid box represents the range of the gridded precipitation data

The annual ring widths of each core and cross-section were measured to the nearest 0.01 mm. Each ring-width measurement series was detrended by fitting a cubic smoothing spline with a 50% cutoff frequency of 200 years to remove non-climatic trends due to age, size, and the effects of stand dynamics (Cook and Briffa, 1990) (Table II). For each site, the index series were prewhitened with low-order autoregressive models to remove persistence. This persistence is presumed to be unrelated to precipitation variability because the

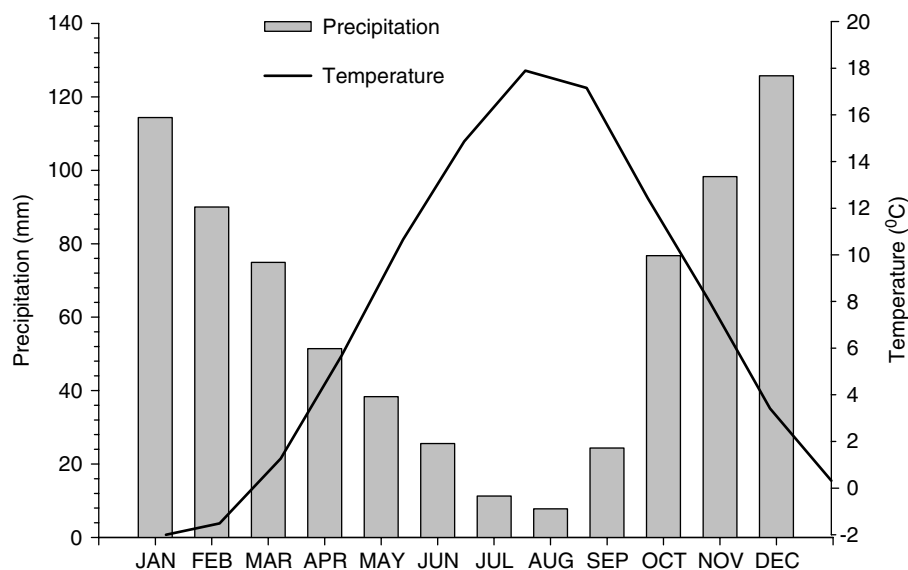


Figure 2. Climogram for Elmali weather station (1968–2000)

Table II. Summary statistics for the nine chronologies from computer program ARSTAN

Site code	Total chronology				Common intervals				
	Standard deviation	Skewness	Kurtosis	1st year SSS > 0.85 ^a	Time span	Total no of years	Mean correlation among radii	1st PC variance (%)	
Su Batan	SUB	0.18	0.09	0.11	1341	1673–1950	278	0.44	50
Aziziye	AZY	0.13	0.01	0.17	1814	1861–2000	140	0.33	38
Dumali Dağ & Göller	DUDGOL	0.19	0.19	-0.15	1864	1903–2000	98	0.44	47
Katrandagi	KAT	0.18	0.16	0.18	1815	1878–2000	123	0.46	49
Göller	GOLJ	0.16	0.14	0.46	1567	1759–2000	242	0.33	37
Kozlu Pinari	KOP	0.15	0.24	0.83	1685	1744–2000	257	0.32	36
Yellic Beli	YEB	0.19	0.15	0.15	1779	1818–2000	183	0.38	43
Elmali	ELMJ	0.19	0.21	0.21	1466	1820–2000	182	0.34	41
Elmali	ELMC	0.19	-0.48	1.47	1522	1648–2000	353	0.56	59

^a SSS is subsample signal strength (Wigley *et al.*, 1984).

precipitation series are not significantly autocorrelated. The indices from individual cores were then combined into a master chronology for each combination of site and species using a biweight robust estimate of the mean (Cook, 1985).

Visual crossdating and computer-based quality control showed such strong similarity between the Dumali Dağ and Göller sites that these *P. brutia* ring-width series were combined into a single chronology.

3.2. Climate data

Gridded precipitation records (5° latitude/longitude) developed by Hulme (1992) were obtained from the Web (<http://www.cru.uea.ac.uk/~mikeh/datasets>). We used the historical monthly precipitation data for 35–40°N, 30–35°E in our regression models. We selected the period 1931 to 1998 for our analysis, because

most of the station records in the area in this data set begin in 1931. Gridded precipitation data were preferred to station data, because the gridded data are better documented and quality controlled and are more suitable for summarizing the large-scale regional variation. To test the agreement between the two sources of data, we compared the gridded precipitation data with an average of seven local climate stations for the period of 1931–98. The correlation between them is high and significant ($p < 0.001$, $r = 0.90$), further indicating that the gridded climate data are representative of the actual regional climate.

3.3. Dendroclimatic reconstruction

As a preliminary step, the relationship between tree-ring indices and monthly and seasonal groupings of gridded temperature and precipitation was investigated with response functions (Fritts, 1976, 1991). Response-function plots (not shown) identify May–June total precipitation as the most appropriate seasonal predictand for reconstruction, as had response function analyses for a much larger region (Hughes *et al.*, 2001: 69).

Two separate reconstructions were developed to accommodate the varying chronology lengths. The first reconstruction uses all nine tree-ring chronologies, with a common interval AD 1776–1998; the second reconstruction uses just the three exceptionally old *J. excelsa* chronologies, with a common interval AD 1339–1998.

The sets of nine and three tree-ring chronologies were transformed to uncorrelated predictors by principal components analysis (PCA) prior to developing a regression equation. This transformation emphasizes the variance in common among the original chronologies (Fritts, 1976; Kutzbach and Guetter, 1980; D'Arrigo and Jacoby, 1991). Predictors for the final reconstruction models were selected by a forward stepwise procedure. The first, third, and eighth PCs, accounting for 43% of the tree-ring variance, were entered as predictors for the first reconstruction, whereas the first and the third PCs, accounting for 58% of the tree-ring variance, were entered as predictors for the second reconstruction. Calibration equations used precipitation data for the period 1931–98, in order to maximize the number of observations and the degrees of freedom used to calculate model significance in the final regression equation. The PRESS procedure was used for cross-validation (Weisberg, 1985; Fritts *et al.*, 1990; Meko, 1997; Touchan *et al.*, 1999). Model stability was also verified using a split-sample procedure (Snee, 1977; Meko and Graybill, 1995) that divided the full period into two subsets of equal length (1931–64 and 1965–98).

3.4. Synoptic climatology analysis

Composites of May–June 500 hPa geopotential height anomalies from the 1968–96 mean were created using National Centers for Environmental Prediction–National Center for Atmospheric Research reanalysis data (Kalnay *et al.*, 1996) for the highest and lowest deciles of reconstructed spring precipitation ($n = 5$) in the period 1948–98.

We used the Jones *et al.* (1997) North Atlantic oscillation (NAO) data (<http://www.cru.uea.ac.uk/cru/data/nao.htm>), which uses differences between the Azores and Stykkisholmur, Iceland, in order to investigate links between the state of the Atlantic ocean–atmosphere system and precipitation in central Turkey. Links between the NAO, winter precipitation over the Mediterranean region, and streamflow in eastern Turkey have been established by other researchers (Cullen and deMenocal, 2000; Glueck and Stockton, 2001; Quadrelli *et al.*, 2001).

3.5. Analysis of wet and dry periods

We summarized short-term May–June drought properties of the 1339–1998 reconstruction by runs analysis (Dracup *et al.*, 1980) using an arbitrary drought threshold of 53.55 mm. This threshold is 80% of the 1931–98 mean observed May–June precipitation. The probability of the maximum drought severity for various drought lengths was estimated by Monte Carlo simulation following a method described more fully by Touchan *et al.* (1999). The method involves counting run lengths and computing run severity for 1000 ‘noise-added’ reconstructions generated by adding random normal noise to the annual reconstruction. Drought severity is defined as the cumulative deficiency of precipitation below the threshold during a given run of consecutive

years below the threshold. In order to provide an alternative summary of the runs analysis, we developed a 5 year moving average for the May–June precipitation reconstruction with an 80% confidence limit derived by Monte Carlo analysis. Analysis of wet periods used an arbitrary threshold of 120% of the 1931–98 mean (80.33 mm).

4. RESULTS AND DISCUSSION

4.1. Chronology

The length of the nine chronologies, the oldest of which are of *J. excelsa*, ranges from 229 years (1772–2000) to 849 years (1152–2000) (Table I and Figure 3). Statistical analyses of each chronology are summarized in Table II. The mean correlation among individual radii at each site, an unbiased estimate of percentage variance in common, summarizes the strength of the common signal. The mean correlation ranges from 0.32 to 0.56. The highest is for Elmali (ELMC) and the lowest is for Kozlu Pinari (KOP); we suspect that the value at KOP is low because the tree species there, *P. nigra*, is less sensitive than the other species to climatic variations.

Some difficulty was found in crossdating some of the juniper and the cedar samples, due to the incidence of locally absent rings. The percentage of absent rings in the juniper and cedar samples is between 0.07–0.15% and 0.11–0.15% respectively. Fisher (1994) reported that *J. excelsa* from Oman has a high proportion of

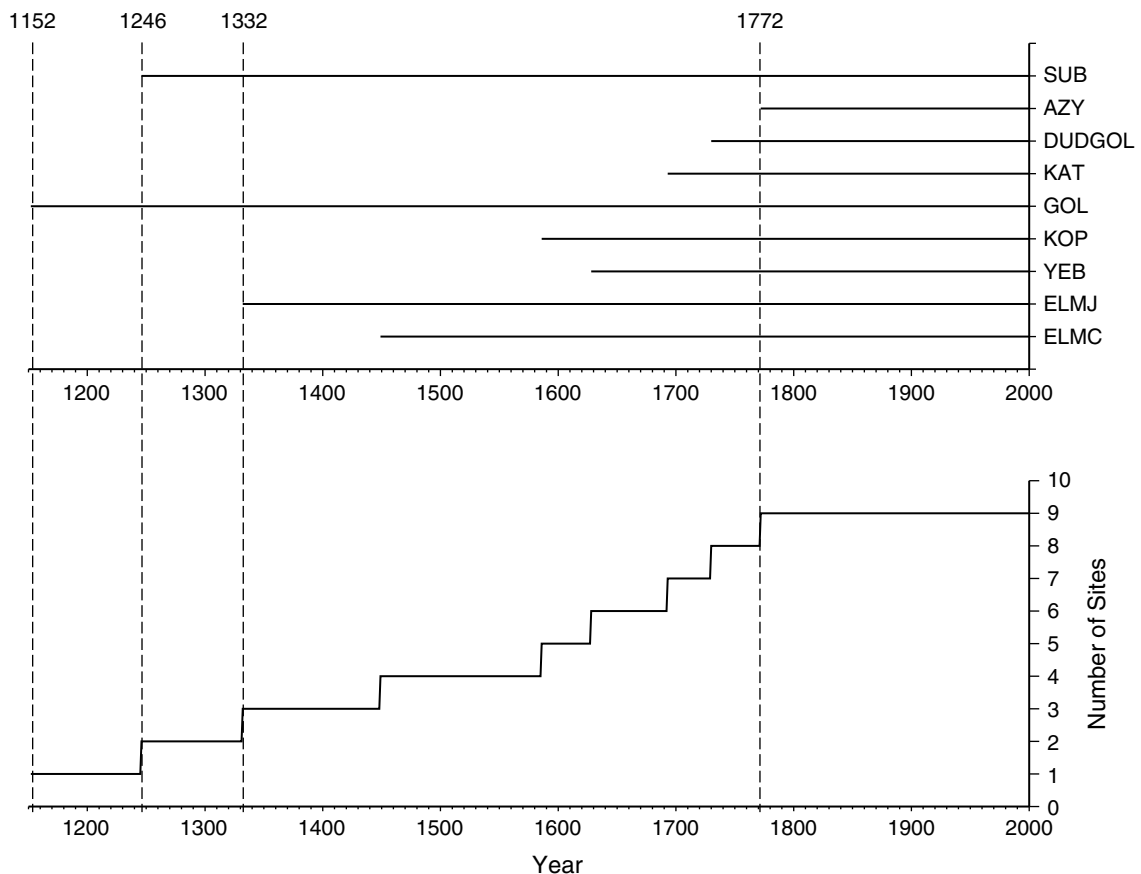


Figure 3. Time coverage of chronologies. Upper panel: each horizontal line marks the time span of the chronology whose letter code appears by the right-hand scale. Lower panel: total number of chronologies in each year

locally absent (8.8%) and false rings. Touchan *et al.* (1999) showed that *Juniperus phoenicia* in southern Jordan had many locally absent rings (0.71%). Based on visual inspection of the samples, absent rings in *Cedrus* are most likely related to the occurrence of fires or to branches broken by heavy snow load. Cedar forms traumatic resin ducts during natural disturbance events (i.e. fire and branches broken by heavy snow).

The average correlation of all pairs of site chronologies is significant ($r = 0.35$, $n = 225$, $p \leq 0.01$). We made use of PCA to capture the regional dendroclimatic signal, as well as to understand how the chronologies filter their respective climatic signals.

4.2. Dendroclimatic reconstruction

The final regression of the 1776–1998 reconstruction obtained from the relationship between the transformed tree-ring data (predictors) and precipitation (predictand) is highly significant ($F = 20.82$, $p \leq 0.0001$) (Figure 4(A)). The regression model for the calibration period is

$$\text{May–June PPT (mm)} = 66.3 - 8.49 \text{ PC1} - 5.51 \text{ PC3} - 8.53 \text{ PC8}$$

The predictor variables account for 47% (adjusted for the degrees of freedom) of the variance in the precipitation data.

The reconstruction equation for the period 1339–1998 is also highly significant ($F = 26.93$, $p \leq 0.0001$) (Figure 4(B)). The regression equation for the calibration period is

$$\text{May–June PPT (mm)} = 67.3 - 12.6 \text{ PC1} + 5.44 \text{ PC3}$$

The predictor variables account for 44% of observed precipitation. Cross-validation using the PRESS procedure indicated that the model performs adequately in estimating precipitation data not used to fit the model ($R^2_{1776-1998} = 0.43$; $R^2_{1339-1998} = 0.39$). The Pearson correlation coefficient between the two reconstructions is 0.91 ($n = 222$, $p \leq 0.0001$). We used the full calibration period (1931–98) for both reconstructions because of the similarity and strength of the derived calibration equations and verification tests of the two subset periods (Table III).

Table III. Results of the statistical calibrations between May through June precipitation and tree growth for both reconstructions

Reconstruction	Calibration period	Verification period	Variable	Coefficient	SD	<i>T</i> -ratio	<i>p</i>	Adjusted R^2	
								for calibration	for verification
1776–1998	1965–98	1931–64	Constant	65.849	2.770	23.770	0.000	0.438	0.467
			PC1	–8.394	1.946	–4.310	0.000		
			PC3	–4.772	3.101	–1.540	0.134		
			PC8	–11.987	5.046	–2.380	0.024		
1339–1998	1965–98	1931–64	Constant	66.870	2.641	25.320	0.000	0.438	0.426
			PC1	–11.561	2.284	–5.060	0.000		
			PC3	4.431	3.574	1.240	0.224		
1776–1998	1931–64	1965–98	Constant	67.826	3.717	18.250	0.000	0.459	0.430
			PC1	–8.899	1.683	–5.290	0.000		
			PC3	–5.826	4.250	–1.370	1.181		
			PC8	–4.646	6.215	–0.750	0.461		
1339–1998	1931–64	1965–98	Constant	67.281	3.716	18.110	0.000	0.409	0.455
			PC1	–13.515	2.785	–4.850	0.000		
			PC3	6.317	4.483	1.410	0.169		

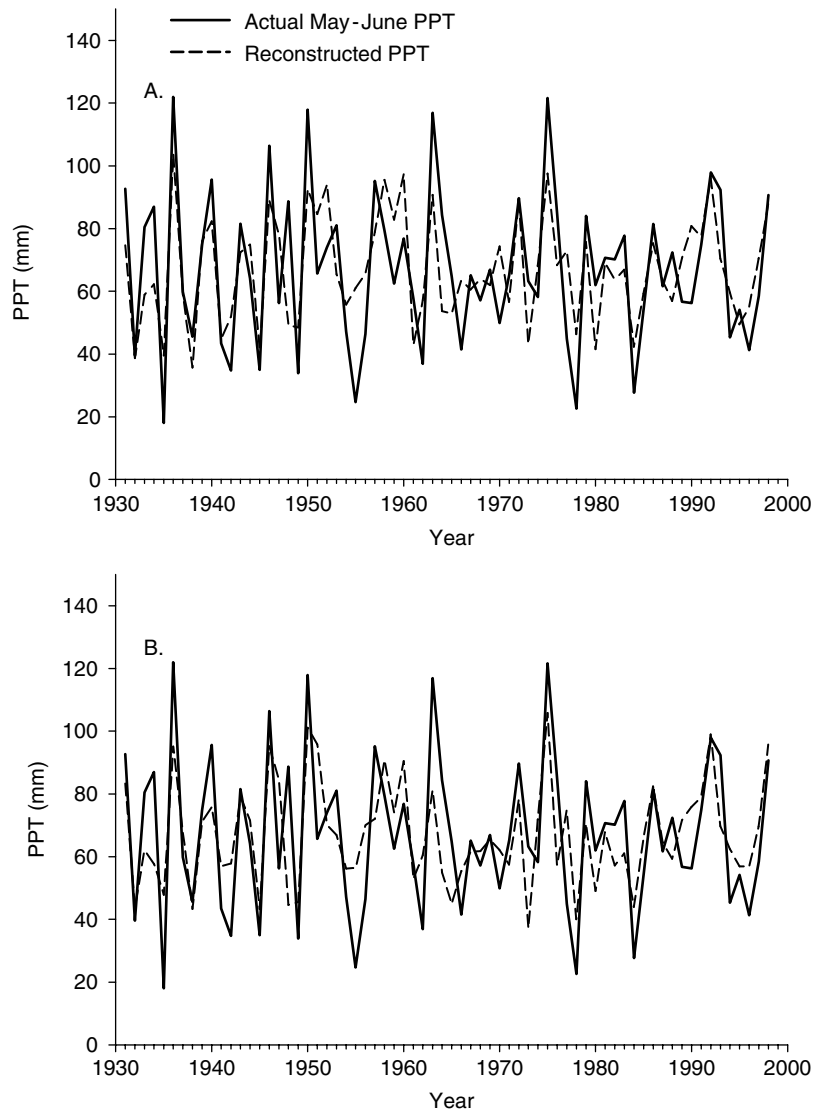


Figure 4. Comparison of actual and estimated May and June precipitation for the 1931–98 calibration period: (A) 1776–1998 reconstruction, based on nine chronologies; (B) 1339–1998 reconstruction, based on three chronologies

4.3. Synoptic climatology analysis

The 500 hPa anomaly pattern for low decile reconstructed spring precipitation years exhibits a pattern of alternating centres of negative and positive anomalies at latitudes north of 60°N, accompanied by alternating centres of positive and negative anomalies between 40–60°N, and positive anomalies over northeastern Africa and the eastern Mediterranean (Figure (5a)). Lower than average 500 hPa heights over most of Europe (exhibiting a sharp gradient over southern Europe), in combination with higher than average 500 hPa heights over northern Africa, yield an enhanced zonal component and slight southwesterly flow anomalies over southern Europe and Turkey. This flow pattern, also characterized by enhanced zonal flow at lower levels (not shown), suggests advection of warm air from North Africa.

The pattern is moderately consistent: four out of five years (1961, 1978, 1980, 1984) exhibit the composite pattern of alternating positive and negative anomaly centres with negative anomalies over Europe, and three of those years also exhibit the combination of negative anomalies over Europe and positive anomalies over

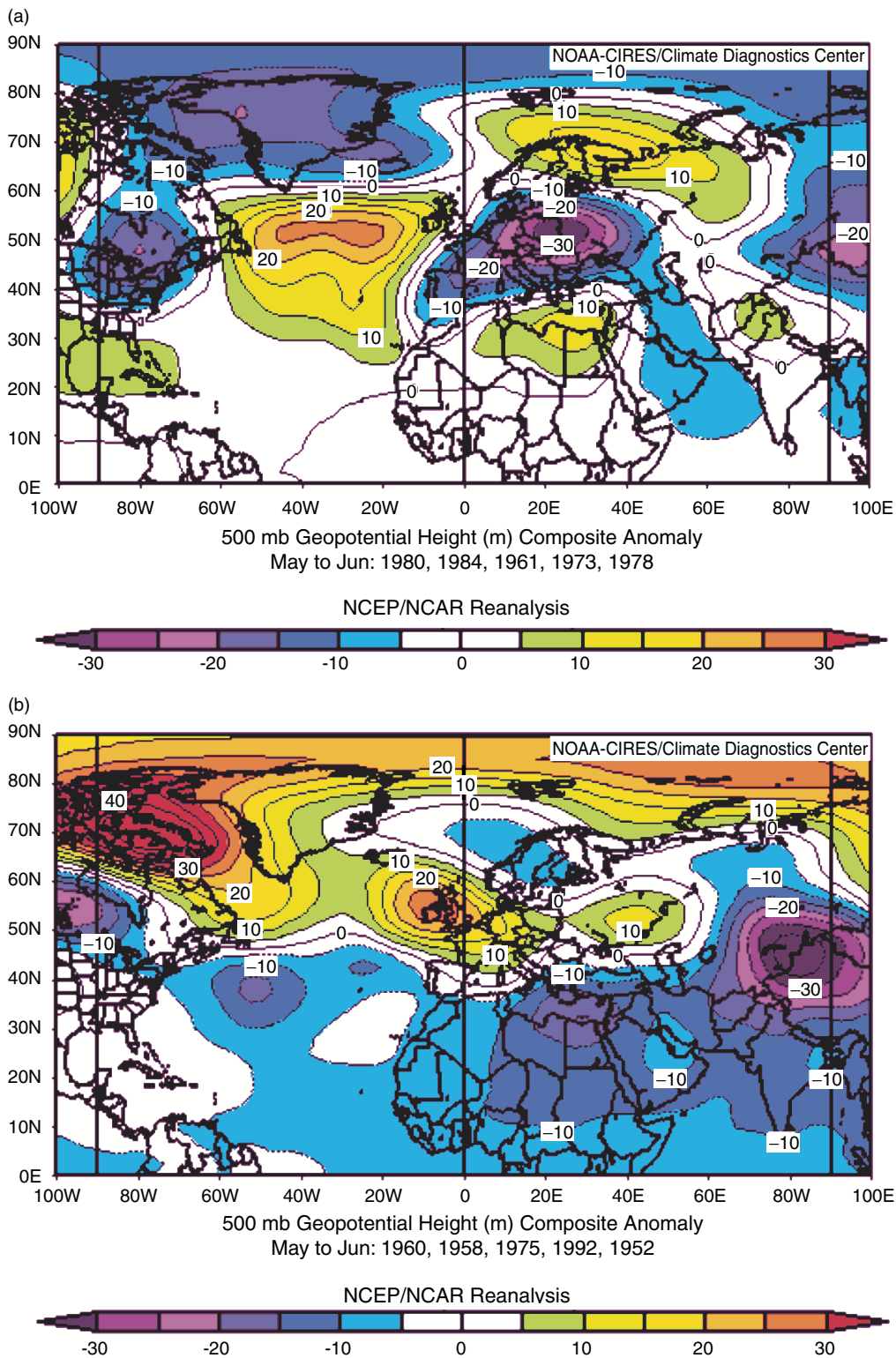


Figure 5. The 500 hPa geopotential height composite anomalies for (a) extremely dry and (b) extremely wet years reconstructed in southwestern Turkey. Heights are expressed as anomalies from the 1968–96 mean. Image provided by the NOAA–CIRES Climate Diagnostics Center, Boulder, Colorado, USA, from their website at <http://www.cdc.noaa.gov/>

northern Africa. Temperature and precipitation composites, averaged from seven surface stations near the chronology sites, exhibit dry and slightly warm conditions during extreme low growth years during the latter half of the 20th century. The association between lower than average 500 hPa heights over Europe and warmer than average temperatures in southwestern Turkey is similar to the association between a deep sea-level pressure (SLP) depression over central and western Europe and high temperatures in the eastern Mediterranean described by Maheras and Kutiel (1999) in their analysis of Mediterranean temperature variations during the last century.

High decile reconstructed spring precipitation year 500 hPa anomalies are lower in magnitude than the low growth decile anomalies; the pattern of circulation anomalies features lower than average heights over much of the region south of $\sim 40^\circ\text{N}$ and higher than average heights over much of Europe (Figure 5b)). Mean 500 hPa winds (not shown) exhibit easterly and northeasterly flow over Turkey and the eastern Mediterranean, whereas the 850 hPa zonal flow is approximately average (westerly) (Figure 5b)). Temperature and precipitation composites suggest that extremely high reconstructed spring precipitation years are characterized by wet and slightly cooler than average conditions. This is consistent with high-level transport of cool air from the European continent, which should provide sufficient cooling to rain out moisture advected from lower latitude sources.

This pattern also exhibits some consistent features in four out of the five years (1952, 1960, 1975, 1992) used to generate the composite. Positive 500 hPa anomalies appear over western and northwestern Europe in four of the five years, and negative 500 hPa anomalies are conspicuous in each year over northern Africa and the eastern Mediterranean. The fact that the high decile reconstructed spring precipitation year 500 hPa anomaly pattern is consistent with above-average precipitation and with Mediterranean 500 hPa PC2 (Quadrelli *et al.*, 2001; their figure 7b and e) for wintertime Mediterranean precipitation suggests the persistence of this winter circulation pattern during wet springs. These results resemble those of Hughes *et al.* (2001) in some respects, and differ in others. In particular, both analyses show negative pressure anomalies over much of Europe in years with dry springs detected by tree rings. Some of the differences between the two analyses may result from differences in the data and methods used. Hughes *et al.* (2001) were able to use a longer period of analysis (1921–90) by using SLP anomalies, which are, however, subject to greater influence by surface features.

4.4. Analysis of dry and wet periods

We restrict the drought analysis to the longer of the two reconstructions (1339–1998) as the statistics are quite similar to those of the 1776–1998 reconstruction. The May–June precipitation reconstruction time series is plotted in Figure 6. The long-term reconstruction for the period of 1339–1998 contains 139 spring-season drought events with a mean interval between them of 4.8 years, which is similar to findings in Jordan (based on October to May precipitation reconstruction) where the average interval between droughts is 4.2 years (Touchan *et al.*, 1999). The maximum interval between spring drought events is 19 years (1848–66). A total of 117 drought events had a duration of 1 year, five drought events had a duration of 2 years, four drought events had a duration of 3 years, and one drought event had a duration of 4 years (1476–79). The single driest spring was 1746 (15.95 mm), and the driest spring for the observed data was 1935 (18 mm). We found that dry periods of 1–2 years were well distributed throughout the record; however, extended dry periods (3–4 years) were not evident during the 16–17th centuries. The single wettest spring was 1827 (127.85 mm). The wettest spring season for the observed data was 1936 (122 mm). Wet periods of 1–2 years were well distributed throughout the record, with the exception of the early to mid 1800s. Extended wet periods were most severe during the 1500s (1532–35) and late 1600s (1688–90).

The Monte Carlo analysis of noise-added reconstructions shows that spring droughts of 6 years or longer are unlikely to occur, since only 11.6% of the 1000 simulations had even one such drought in the 659 year record (Figure 7). Touchan *et al.* (1999) reported that Monte Carlo analysis indicated a lower than 50% chance that southern Jordan has experienced drought longer than 5 years in the past 400 years. In this study, all the 1000 noise-added simulations have at least one 3 year drought. The maximum severity of a 3 year spring drought is considerably greater in a long-term context (74 mm deficit) than suggested by the short observed records (42 mm deficit).

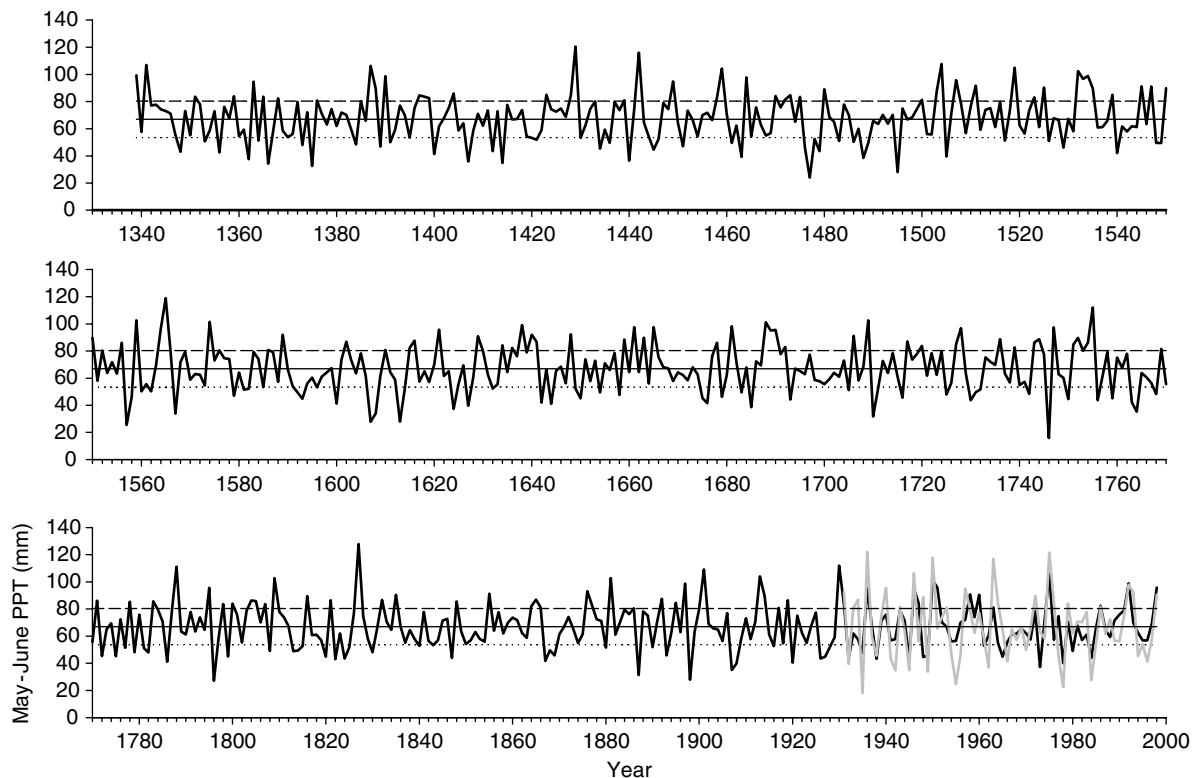


Figure 6. Time series plot of reconstructed May to June precipitation, 1339–1998. Horizontal solid line is the mean of the observed data. Horizontal dashed line is the arbitrary threshold of 120% of the 1931–98 mean May–June precipitation (80.33 mm). Horizontal dotted line is the arbitrary threshold of 80% of the 1931–98 mean May–June precipitation (53.55 mm). The instrumental record is in grey

The May–June 5 year moving average precipitation reconstruction indicates multi-year and decadal variation in spring precipitation. Extended dry periods were absent from the first half of the 16th century (Figure 8). Wet periods were more severe prior to 1800; in fact, all of the wettest 5 year periods occurred prior to 1756. The driest 5 year spring mean is 1475–79 (50 mm); however, confidence interval calculations indicate only a 10% probability that this 5 year mean was as low as 40 mm. The wettest 5 year spring mean is 1751–55 (90.7 mm); confidence interval calculations indicate a 10% probability that this wet period was as high as 100 mm. The lowest 5 year spring mean in the instrumental record (1941–45) is slightly higher (51.75 mm) than the 5 year reconstructed mean for 1475–79. The highest 5 year spring mean in the instrumental data is 1972–76 (80.61 mm).

4.5. Links with the NAO

In order to establish whether our spring precipitation reconstructions exhibited links with large-scale atmospheric circulation in the Northern Hemisphere, we analysed multiple correlations between our spring precipitation reconstructions, instrumental spring precipitation, and various lags of monthly and seasonal values of the NAO, for the period 1900–97. We found no significant correlations ($p \leq 0.05$) between May–June instrumental precipitation and the NAO. The highest correlations were between concurrent March–May NAO and May–June instrumental precipitation ($r = 0.19$, $p = 0.12$) and concurrent April NAO and May–June instrumental precipitation ($r = 0.21$, $p = 0.09$). Correlations between reconstructed May–June precipitation and NAO (1865–1997) were also of low magnitude for concurrent spring and April NAO ($r_{1339-1998-AMJ} = 0.18$, $p = 0.04$; $r_{1339-1998-Apr} = 0.17$, $p = 0.05$; $r_{1776-1998-AMJ} = 0.28$, $p = 0.01$;

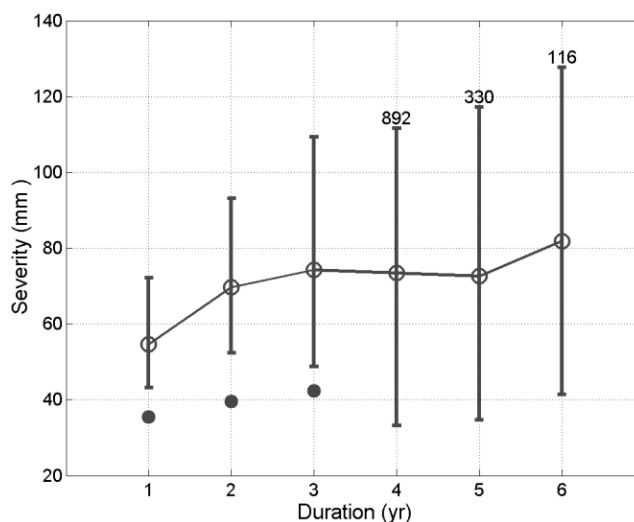


Figure 7. Monte Carlo summary of likely severity of most severe droughts of various duration as inferred from noise-added tree-ring reconstructions. Circle and whiskers mark median, 5th, and 95th percentiles of severity of most severe n -year droughts in reconstructions. Solid dots mark severity of most severe n -year droughts in the observed precipitation series, 1931–98. Results based on 1000 simulations of random noise added to the 1339–1998 reconstruction. Severity defined as cumulative deficit below threshold (see text). Number of simulations with an n -year drought annotated (e.g. 892) when not all 1000 simulations have at least one such drought

$r_{1776-1998-Apr} = 0.18$, $p = 0.04$). Correlations with winter NAO were weak but negative ($r_{1339-1998-DJFM} = -0.19$, $p = 0.03$; $r_{1776-1998-DJFM} = -0.15$, $p = 0.08$). However, concurrent spring correlation values proved to be somewhat more robust during the period from 1931 to present ($r_{1339-1998-AMJ} = 0.23$, $p = 0.06$; $r_{1339-1998-Apr} = 0.37$, $p < 0.01$; $r_{1776-1998-AMJ} = 0.31$, $p = 0.01$; $r_{1776-1998-Apr} = 0.37$, $p < 0.01$). Although we are loathe to overinterpret the results of these weak correlations, positive correlations with the concurrent NAO would indicate lower than average spring precipitation when circulation typically favours storm tracks to the north of the Mediterranean, a result that is the opposite of our expectations. Such results point to alternate favourable storm tracks, e.g. paths that originate from southwestern Russia or the Balkans and cross the Black Sea (Alpert *et al.*, 1990; Karaca *et al.*, 2000) during years with high values of spring NAO.

5. CONCLUSIONS

Tree rings provide a valuable natural archive to study past climate variability in the eastern Mediterranean region. Our reconstructions are the first precisely dated and well-replicated annual resolution reconstructions of spring precipitation for southwestern Turkey. Our analysis of spring drought parameters provides natural-resource managers with a better understanding of the duration, intensity, and frequency of drought during the last 660 years, as well as a more complete understanding of the potential range of catastrophic climatic anomalies, e.g. extended dry and wet periods.

Multi-year to decadal variations in spring precipitation are evident from our reconstructions. According to our extended reconstruction, the longest period of drought during the past six centuries is 4 years (1476–79); only one drought of this duration occurred during the past 660 years. Droughts of 3 years in duration occurred only during the 18th–20th centuries. Monte Carlo analysis showed that drought periods longer than 5 years are unlikely to happen in southwest Turkey. The absence of extended drought during the 1500s–1600s, and the occurrence of extended wet periods during these centuries suggest a possible shift in spring climate during this period. Based on analysis of synoptic climatology associated with extreme dry and wet years during the 20th century, we believe that dry springs are characterized by warm conditions and southwesterly upper-level flow over the eastern Mediterranean, whereas wet springs are likely characterized by cooler than average conditions brought on by anomalous upper-level flow from the European continent and mean westerly flow

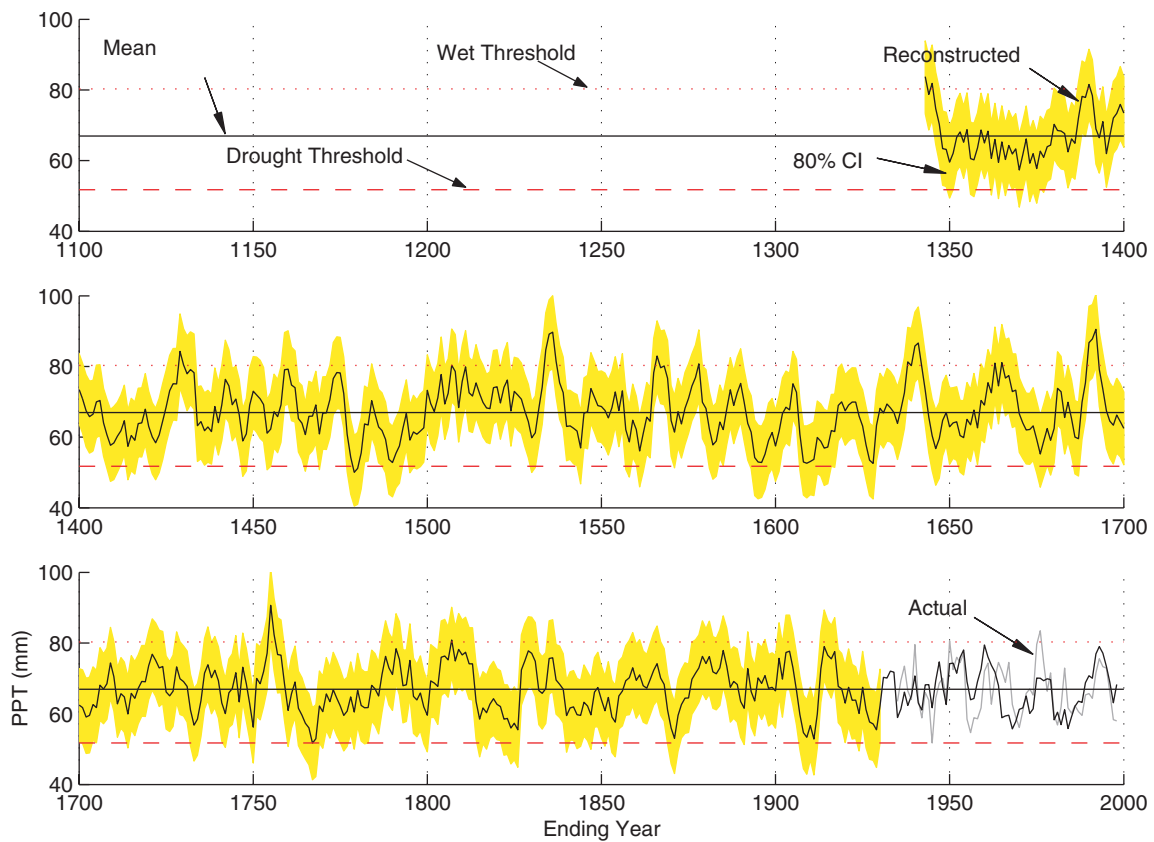


Figure 8. Five-year running means of reconstructed May–June precipitation for southwestern Turkey. Values are plotted at the last year of each 5 year period for the 1339–1998 reconstruction and the 1931–98 observed data. Uncertainty in reconstructed values is shown by an 80% confidence interval (shaded) derived by Monte Carlo analysis

lower in the troposphere. We found a weak negative correlation between winter NAO and reconstructed spring precipitation and positive correlation between April NAO and reconstructed spring precipitation. The lack of strong correlation might be due either to the transition in atmospheric circulation between May and June or because stronger links with the NAO are found in eastern Turkey (Cullen and deMenocal, 2000).

During the summer of 2001 we performed fieldwork to increase the sample depth of our collections for the early part of the record, and to expand the geographic region of our network of well-replicated chronologies. These collections should allow us to create more accurate and spatially extensive reconstructions in order to understand past climate variations in this region better. Our reconstructions provide insights, to a first approximation, into variations of vegetation growth in the eastern Mediterranean. As trees are natural integrators of both temperature and precipitation, an intriguing avenue for our future research is to attempt reconstruction of potential evapotranspiration (e.g. Palutikof *et al.*, 1994), a key variable for agriculture and water-resource management.

ACKNOWLEDGEMENTS

We thank the Ministry of Forestry, Southwest Anatolia Forest Research Institute (SAFRI), specifically Mr Yusuf Cengiz, the Director of SAFRI, for his great help and support and making this study possible. We thank Maher Qishawi, Necati Bas, Erdogan Uzun, and Galip Yanik for their valuable assistance in the field, Candice Marburger for her assistance in sample preparation and measurement, and Richard Holmes for his

advice and suggestions. Funding was provided by the US National Science Foundation, Earth System History (grant Nos 0075956 and 0080834).

APPENDIX A

Aziyiye (AZY) and Su Batan (SUB): the soil surface is rocky (30–60%) and the parent materials consist of sand, silt, and marl deposits (Pamir, 1964; Cepel and Kalay, 1992). The parent material at Dumali Dağ (DUD) and Katrandagi (KAT) is hard bluish limestone, and 40% of the soil surface is covered with rock. The soil depth is around 20 cm. The parent material for Göller (GOL) is volcanic rocks with 40–85% of the surface covered with rocks. The Elmali area is primary calcareous in structure with shallow soil development (less than 1 m depth). Soil suitable for root development and tree growth is possible because the surface bedrock is cracked horizontally, allowing the deposit of good organic soil (Turkish Ministry of Forestry, 1997). The parent material for Kozlu Pinari (KOP) and Yellic Beli (YEB) is hard crystallized cracked limestone. The soil is red–brown sandy and more than 1 m in depth.

REFERENCES

- Alpert P, Neeman BU, Shay-El Y. 1990. Intermonthly variability cyclone tracks in the Mediterranean. *Journal of Climate* **3**: 1474–1478.
- Akkemik Ü. 2000. Dendroclimatology of Umbrella pine (*Pinus pinea* L.) in Istanbul, Turkey. *Tree-Ring Bulletin* **56**: 17–23.
- Bannister B. 1970. Dendrochronology in the Near East: current research and future potentialities. In *Proceedings of the seventh International Congress of Anthropological and Ethnological Sciences*, vol. 5; 336–340.
- Cepel N, Kalay Z. 1992. Antalya Orman Yetisme Bölgesinin Ekolojik Özellikleri, Türkiye Akdeniz Bölgesi Ormanlar I ve Ormancılığına İlişkin Bilimsel Yaklaşımlar, Istanbul University Faculty of Forestry.
- Cook ER. 1985. A time series analysis approach to tree-ring standardization. Unpublished PhD dissertation, University of Arizona, Tucson.
- Cook ER, Briffa KR. 1990. A comparison of some tree-ring standardization methods. In *Methods of Dendrochronology: Applications in the Environmental Sciences*, Cook ER, Kairiukstis LA (eds). Kluwer Academic Publishers: Boston; 153–162.
- Cullen HM, deMenocal PB. 2000. North Atlantic influence on Tigris–Euphrates streamflow. *International Journal of Climatology* **20**: 853–863.
- D'Arrigo RD, Jacoby GC. 1991. A 1000-year record of winter precipitation from northwestern New Mexico, USA: a reconstruction from tree-rings and its relation to El Niño and the southern oscillation. *The Holocene* **1**(2): 95–101.
- Dracup J, Lee KS, Paulson EG. 1980. On the definition of droughts. *Water Resources Research* **16**(2): 297–302.
- Fisher M. 1994. Is it possible to construct a tree-ring chronology for *Juniperus excelsa* (bieb) subsp. *Polycarpus* (K. Koch), Takhtajan from the Northern Mountains of Oman? *Dendrochronologia* 119–127.
- Fritts HC. 1976. *Tree Rings and Climate*. Academic Press: London.
- Fritts HC. 1991. *Reconstruction of Large-scale Climatic Patterns from Tree-ring Data*. The University of Arizona Press: Tucson.
- Fritts HC, Guiot J, Gordon GA, Schweingruber F. 1990. Methods of calibration, verification, and reconstruction. In *Methods of Dendrochronology: Applications in the Environmental Sciences*, Cook ER, Kairiukstis LA (eds). Kluwer Academic Publishers: Boston; 163–217.
- Gassner G, Christiansen-Weniger F. 1942. Dendroklimatologische Untersuchungen über die Jahresringentwicklung der Kiefer in Anatolien. *Nova Acta Leopoldina* **12**: 1–134.
- Glueck MF, Stockton CW. 2001. Reconstruction of the North Atlantic oscillation, 1429–1983. *International Journal of Climatology* **21**: 1453–1465.
- Hughes MK, Kuniholm PI, Garfin GM, Latini C, Eischeid J. 2001. Aegean tree-ring signature years explained. *Tree-Ring Research* **57**(1): 67–73.
- Hulme M. 1992. A 1951–80 global and precipitation climatology for the evaluation of general circulation models. *Climate Dynamics* **7**: 57–72.
- Jones PD, Jónsson T, Wheeler D. 1997. Extension to the North Atlantic oscillation using early instrumental pressure observations from Gibraltar and south-west Iceland. *International Journal of Climatology* **17**: 1433–1450.
- Kalnay E, Kanamitsu M, Kistler R, Collins W, Deaven D, Gandin L, Iredell M, Saha S, White G, Woollen J, Zhu Y, Chelliah M, Ebisuzaki W, Higgins W, Janowiak J, Mo KC, Ropelewski C, Wang J, Leetmaa A, Reynolds R, Jenne R, Joseph D. The NCEP/NCAR reanalysis 40-year project. *Bulletin of the American Meteorological Society* **77**(3): 437–471.
- Karaca M, Deniz A, Tayanc M. 2000. Cyclone track variability over Turkey in association with regional climate. *International Journal of Climatology* **20**: 1225–1236.
- Kuniholm PI. 1990. Archaeological evidence and non-evidence for climatic change. *Philosophical Transactions of the Royal Society of London, Series A* **330**: 645–655.
- Kuniholm PI. 1994. Long tree-ring chronologies for the eastern Mediterranean. In *Proceedings of the 29th International Symposium on Archaeometry*.
- Kuniholm PI, Striker CL. 1987. Dendrochronological investigations in the Aegean and neighboring regions, 1983–1986. *Journal of Field Archaeology* **14**: 385–398.
- Kutzbach JE, Guetter PJ. 1980. On the design of paleoenvironmental data networks for estimating large-scale patterns of climate. *Quaternary Research* **14**: 169–187.

- Luterbacher J, Schmutz C, Gyalistras D, Xoplaki E, Wanner H. 1999. Reconstruction of the monthly NAO and EU indices back to AD 1675. *Geophysical Research Letters* **26**(17): 2745–2748.
- Maheras P, Kutiel H. 1999. Spatial and temporal variations in the temperature regime in the Mediterranean and their relationship with circulation during the last century. *International Journal of Climatology* **19**: 745–764.
- Meko DM. 1997. Dendroclimatic reconstruction with time varying subsets of tree ring indices. *Journal of Climate* **10**: 687–696.
- Meko DM, Graybill DA. 1995. Tree-ring reconstruction of Upper Gila River discharge. *Water Resources Bulletin* **31**(4): 605–616.
- Palutikof JP, Goodess CM, Guo X. 1994. Climate change, potential evapotranspiration and moisture availability in the Mediterranean Basin. *International Journal of Climatology* **14**: 853–869.
- Pamir MH. 1964. Geological Map of Turkey, General Directorate of Map, Ankara.
- Quadrelli R, Pavan V, Molteni F. 2001. Wintertime variability of Mediterranean precipitation and its links with large-scale circulation anomalies. *Climate Dynamics* **17**: 457–466.
- Snee RD. 1977. Validation of regression models: methods and examples. *Technometrics* **19**: 415–428.
- Stokes MA, Smiley TL. 1968. *An Introduction to Tree-Ring Dating*. University of Chicago Press.
- Swetnam TW, Thompson MA, Sutherland EK. 1985. Using dendrochronology to measure radical growth of defoliated trees. *USDA Forest Service Agricultural Handbook*, No. 639, 39 pp.
- Touchan R, Meko DM, Hughes MK. 1999. A 396-year reconstruction of precipitation in southern Jordan. *Journal of the American Water Resources Association* **35**(1): 45–55.
- Turkish Ministry of Forestry. 1997. *Forest Management Plans for Mediterranean Region*. Forest Service, Antalya.
- Turkish General Directorate of Meteorology. 2001. Weather Station Databanks of Turkish General Directorate of Meteorology, Ankara.
- Weisberg R. 1985. *Applied Linear Regression*, John Wiley and Sons: New York.
- Wigley TML, Briffa KR, Jones PD. 1984. On the average value of correlated time series, with applications in dendroclimatology and hydrometeorology. *Journal of Climate and Applied Meteorology* **23**: 201–213.